CZECH TECHNICAL UNIVERSITY IN PRAGUE

Faculty of Nuclear Sciences and Physical Engineering

Department of Physics

Research Project

Pixel detectors for electron microscopy

Bc. David Horák

Supervisor: Ing. Mária Čarná

Prague, 2014

ČESKÉ VYSOKÉ UČENÍ TECHNICKÉ
V PRAZE
Fakulta jaderná a fyzikálně inženýrská
Katedra fyziky

Výzkumný úkol

Pixelové detektory pro elektronovou mikroskopii

Bc. David Horák

Vedoucí práce: Ing. Mária Čarná

Praha, 2014

Prohlášení:

Prohlašuji, že jsem svůj výzkumný úkol vypracoval samostatně a použil jsem pouze podklady (literaturu, software, atd.) uvedené v přiloženém seznamu.

Nemám závažný důvod proti užití tohoto školního díla ve smyslu § 60 Zákona č.121/2000 Sb., o právu autorském, o právech souvisejících s právem autorským a o změně některých zákonů (autorský zákon).

V Praze dne ....

David Horák

Acknowledgement

I would like to express my gratitute to all who supported me during the creation of this work. I am very grateful to my supervisor Ing. Mária Čarná, for her willingness, patience, professional feedback and language corrections. I would also like to thank Ing. Michal Marčišovský for his valuable guidance, technical support and helpful consultations. Last but not least, please allow me to thank the Institute of Physics Academy of Sciences of the Czech Republic for its cooperation, especially to Dr.rer.nat. Lukáš Palatinus.

Contents

List of Figures

Chapter 1

Introduction

Electron microscopy plays an important role in understanding of the structure of biological samples, material research and nanotechnologies. This research project tries to propose a better method of image recording based on the Medipix2 detector.

The first chapter discusses the properties of an electron, its interactions with matter and related effects. The characteristics of transmission and scanning electron microscope and the basics of electron microscopy are described in the next chapter. The following chapter describes the working principles of semiconductor detectors and pixel detector fabrication, and one subchapter is dedicated to a hybrid-pixel detector Medipix2, its layout, readout hardware and software. The final chapter presents the results of using the Medipix2 detector in a common transmission electron microscope, describes related issues and corrections of the image, which was obtained by a hexagon-pixel sensor layout.

Chapter 2

Interaction of Electrons with Matter

2.1 Electron and Its Properties

Electron is an elementary particle with a negative charge $e = -1,602 \times 10^{-19}$ C and its rest mass is approximately $m_0 = 511\,\mathrm{keV/c^2}$.

Early in the 20th century, Louis de Broglie proposed that wavelength λ of a particle with momentum p is given by

$$\lambda = \frac{h}{p}, \tag{2.1}$$

where $h = 6,626 \times 10^{-34}\,\mathrm{J \cdot s}$ is the Planck constant. The wavelength of an electron accelerated in an electric field V can be calculated according to

$$\lambda = \frac{h}{\sqrt{2m_0\mathrm{eV}}}. \tag{2.2}$$

However, for the acceleration voltage commonly used in electron microscopy, relativistic effects must be included:

$$\lambda = \frac{h}{\sqrt{2m_0eV\left(1 + eV/2m_0c^2\right)}}. \tag{2.3}$$

Several values of the calculated wavelength of electrons depending on the acceleration voltage commonly used in electron microscopy can be seen in Table 2.1.

V[kV]	λ[pm]
100	3,7
200	2,5
300	1,9

Table 2.1: Wavelength of electrons depending on the acceleration voltage

Waves in an electron beam can be either coherent or incoherent. Waves, that have the same wavelength and are in phase with each other, are called coherent and those that are not, such as sun rays, are called incoherent. Waves also interact with each other, which can results in two extreme cases - constructive interference and destructive interference. In the former, waves are completely in phase and the resulting magnitude of the wave is the sum of both magnitudes, in the latter they are exactly out of phase and waves cancel each other out.

2.2 Electron Interaction with Matter

When a fast electron hits a material (such as a specimen in the electron microscope), different interactions may occur, as is shown in Figure 2.1. In principle, there are two types of interactions - elastic or inelastic.

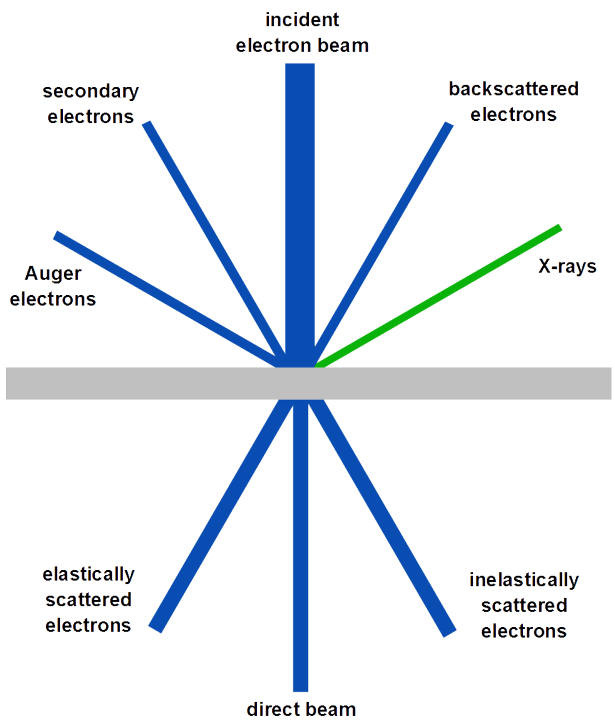

Figure 2.1: Interactions of electrons in matter

2.2.1 Elastic Interactions

In elastic interactions, no energy is transferred from the electron to the material. The electron has its original kinetic energy after interaction.

Incoherent Scattering

An electron penetrating into the atom is attracted by the Coulombic field F of the nucleus

$$F = \frac{1}{4\pi\varepsilon_0}\frac{Ze^2}{r^2}, \tag{2.4}$$

where ε_0 is the dielectric constant, Ze is the charge of the nucleus and r is the distance between the electron and nucleus. The closer the electron is to the nucleus, the larger the F and consequently the scattering angle is. When the electron is close enough to the nucleus, the so-called back-scattered electrons can occur.

The probability that an electron interacts depends on the interaction cross section σ. The total cross section σ_T is the sum of elastic σ_{el} and inelastic σ_{inel} cross section:

$$\sigma_T = \sigma_{el} + \sigma_{inel}. \tag{2.5}$$

The angular distribution of scattered electrons is described by the differential cross section $d\sigma/d\Omega$.

As can be seen from Eq. 2.4, the Coulomb force increases with increasing atomic number Z, this means that the high-Z material scatters electrons more than the low-Z material. Based on this phenomenon, the mass contrast method is used in electron microscopy. Another effect is the so-called thickness contrast. The number of scattered electrons is proportional to the path of the electron in material.

Coherent Scattering at Crystals

If electrons with a certain wavelength λ pass through the crystal, then coherent scattering takes place. All atoms act as scattering centers that deflect the incoming electron. Because the spacing between the atoms is regular, a constructive interference in certain direction happens and diffracted beams are generated. This phenomenon is called the Bragg diffraction.

In analogy to the Huygens principle describing the diffraction of light, a general formula that is also valid for electrons, X-rays and neutrons can be derived. It is called the Bragg equation:

$$2d\sin(\Theta) = n\lambda. \tag{2.6}$$

From this equation, a scattering angle Θ can be obtained, knowing the distance between the lattice planes d. For example, for $d = 0,2$ nm and wavelength $\lambda = 1,9$ pm, a scattering angle $\Theta = 0°16'$ can be calculated, thus diffraction angles in electron diffraction are quite small.

2.2.2 Inelastic Interactions

If the energy of an electron is reduced after an interaction with matter, a so-called inelastic interaction has occurred. The energy transferred to the specimen can cause different effects to occur, such as X-rays, Auger electrons and secondary electrons.

Auger Electrons

Ionization of an atom can leave a vacancy in an inner shell. This unstable configuration result in filling the vacancy with an electron from a higher shell. The excess energy of that electron is transferred to a higher shell electron, which can receive enough energy to be ejected as is shown in Fig. 2.2. This ejected electron is called the Auger electron.

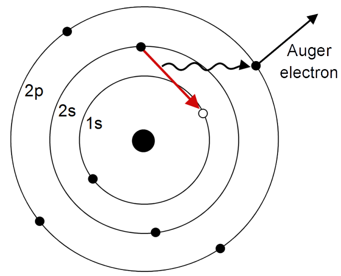

Figure 2.2: A diagram of an Auger electron emission

Because this process is determined by the electronic structure, the energy of the Auger electron is similar to that of the characteristic X-rays and corresponds to the energy difference between atom shells. This energy is in the range between 100 eV and a few 1000 eV [7]. These electrons are heavily absorbed in the material, thus Auger spectroscopy can be used to examine the specimen surface.

Secondary Electrons

Secondary electrons (SE) are generated by other types radiation. They are located in the valence or conduction band; therefore, they need only a small energy transfer to be ejected into the vacuum. A typical energy of the SE is below 50 eV, so like Auger electrons, they are used in scanning electron microscopy for the surface topography of a specimen.

Chapter 3

Introduction into Electron Microscopy

Electron microscopy plays an important role in understanding of the structure of biological samples, material research and nanotechnologies. As was shown in Chapter 1, the wavelength of 200 keV electrons is 2,5 pm. Because this wavelength is comparable to the atomic dimensions, electrons can be used as a probe to the microworld.

3.1 Transmission Electron Microscope

The original form of an electron microscope, created by German physicists Ernst Ruska and Max Knoll in 1931, uses an electron beam to penetrate a thin specimen and then electrons are imaged as in the light microscope. This is a concept of the so-called transmission electron microscope (TEM), which can be seen in Fig. 3.1.

3.1.1 The Electron Gun

An electron gun is an electrical device that produces a narrow, collimated electron beam with a precise kinetic energy. There are several types of electron guns operating on different physical principles.

Thermionic emission

Thermionic emission is the emission of electrons from a hot surface of a cathode. It is usually a V-shaped filament made of tungsten, that emits electrons into the surrounding vacuum at a temperature of about $2700\,K$.

A current density J_e at a source temperature T is expressed by the Richardson-Dushman equation

$$J_e = AT^2 \exp(-\frac{\phi}{kT}), \tag{3.1}$$

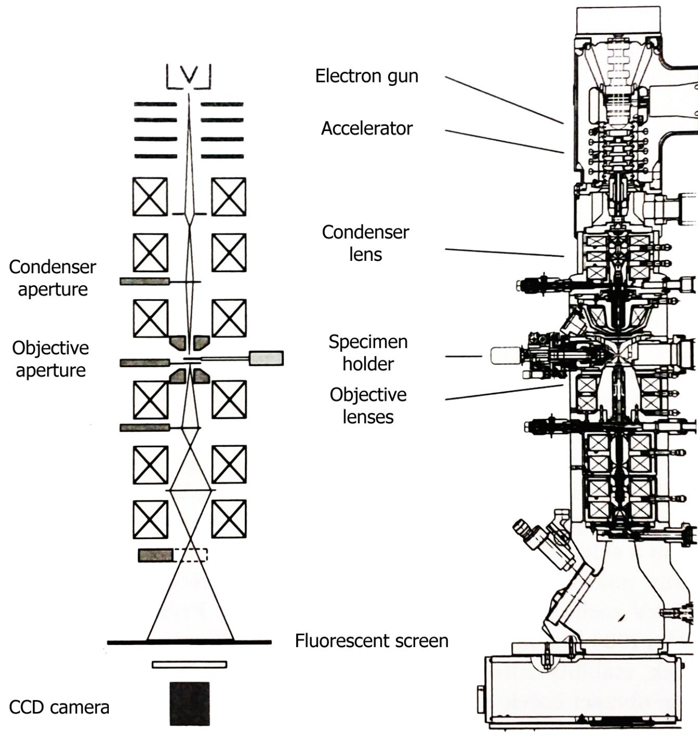

Figure 3.1: A schematic diagram of the transmission electron microscope

where A is the Richardson constant, which depends on the cathode material, k is the Boltzmann constant and ϕ is the work function of the material.

Schottky emission

The thermionic emission can be increased by applying an electrostatic field to the cathode surface. The electric field lowers the surface barrier by an amount of $\Delta\phi$. This is known as the Schottky effect and it typically increases the current density by a factor of 10. [4] After some technological improvement, this is the most used type of electron source.

Field emission

If the electrostatic field at the tip of a cathode is high enough, electrons can escape through the surface barrier by tunneling. This process is known as the field emission.

The tip is made sufficiently sharp, so electrons are emitted from an extremely small area; therefore, an electron beam can be well focused. Thermal excitation is not required, hence this tip can be operated at a room temperature (the process is sometimes called cold field emission); however, an ultra-high vacuum (10^{-8} Pa) is required.

3.1.2 Electron Acceleration

After emission, electrons are accelerated by means of an electric field parallel to the optic axis. This electric field is generated by a potential difference between the cathode and anode which usually consist of a metal plate containing a central hole through which the electron beam passes. Because many of the accelerated electrons are absorbed in the anode and only around 1% passes through, the beam current is typically 1% of the emission current. Most modern TEMs use an electron accelerating voltage between 100 kV and 300 kV [5].

3.1.3 Lens System

Accelerated electrons can be focused by electrostatic or magnetic lenses. Electron microscopes use mainly magnetic lenses due to the smaller imaging defects.

Magnetic lenses

To obtain focusing, an axial symmetry field is needed. The force F acting on electrons with a velocity v and with a charge e in the magnetic field B is called the Lorentz force and is given by

$$\overrightarrow{F} = -e\left(\overrightarrow{v} \times \overrightarrow{B}\right). \tag{3.2}$$

By analyzing this equation, one can find that for an electron traveling along the coil axis there are no deviations of the ray path from a straight line. However, for non-axial trajectories, the motion of the electron is more complicated and a rotation effect occurs.

3.1.4 The Specimen Stage

A specimen in the TEM is always circular with a diameter of 3 mm and thin enough (around 100 μm) to allow electrons to be transmitted through. It is necessary to avoid any undesirable drift or vibration. To allow the specimen to be inserted into the microscope without introducing air, there is an airlock. It is a small chamber where a specimen is placed and which is evacuated before the specimen enters the TEM volume. There are two basic designs of the specimen stage: side-entry and top-entry.

With a side-entry holder, the specimen is placed in a small bore near the tip of a metal rod. The airlock-evacuation valve and vacuum valve are activated by rotation of the holder about its axis.

The top-entry holder consist of a cartridge with a drilled bore in which a specimen is loaded. Unlike the previous design, the cartridge is inserted into the airlock with a bore perpendicular to the optic axis.

3.1.5 Electron Imaging System

A human eye is not sensitive to electrons; therefore, it is necessary to convert the electron image to a visible form. For this purpose, a phosphor screen is used. It consist of a metal plate covered with a thin layer of phosphor material, most commonly zinc sulfide (ZnS). The screen is used mainly for focusing an image. The viewing window is made of a high lead content glass to absorb the x-rays that are produced when electrons interacts. Optical binoculars are often mounted outside the window to provide further magnification. However, recording of the image is usually necessary.

Photographic Film

To permanently record a created image, a photographic film can be used. It has a layer of a silver halide emulsion, similar to that in a black and white photography. Electrons, as well as photons, cause chemical changes that can be shown by immersion in a developer solution. A high resolution and a wide field of view are the main advantages of the photographic film. However, their disadvantages are saturation at a high radiation dose and development in a dark room.

Imaging Plates

In contrast to the photographic film, the electron image is recorded in a layer of crystals embedded in resin. Instead of chemical development, the image is scanned by a special scanner and then cleared in the visible light. The advantage of the imaging plate is great sensitivity at low electron rate and high dynamic range, but the image is not immediately available for viewing.

CCD Camera

Nowadays, almost all electron microscopes are equipped with electronic image-recording devices, especially CCD (charge-coupled device) sensors. Their principle of operation will be discussed in the next chapter. Because CCDs can be easily damaged by electrons, they are fitted with a YAG (yttrium aluminium garnet) scintillator that converts electrons to visible light. The recorded image can be immediately displayed on a monitor screen and easily processed on the computer.

3.1.6 Vacuum System

Electrons are strongly scattered by gas molecules, so it is essential to remove most of the air from the inside of an electron microscope. Additionally, the electron gun requires a sufficiently good vacuum. Also, a reduction of specimen contamination is desirable. The electron vacuum system usually consist of several different types of vacuum pumps.

A rotary vane pump (Fig. 3.2) contains a rotating assembly driven by an electric motor. The internal vanes are separated by a spring, so they are pressed against the inside wall of the pump. The interior of the pump is lubricated with oil to reduce friction, to cool and to provide a seal. The rotation axis is misalignment from the axis of the pump interior, so that a gas can be draw from the inlet tube and pushed out in the outlet tube equipped with a return valve. The rotary pump is able to provide vacuum with a pressure of about 1 Pa.

Another type of vacuum pump used in TEM is a diffusion pump (Fig. 3.3). At the base of the pump, an electrical heater causes a special oil to boil. The oil vapor rises and is deflected downwards by a baffle assembly. The oil molecules collide with air molecules and then condense back into a liquid on the cooled walls. Air molecules are released and pumped away by the rotary pump. Diffusion pumps usually operate in the range of $10\,\mathrm{Pa} - 10^{-7}\,\mathrm{Pa}$.

There are several other types of vacuum pumps used in electron microscopes. A turbomolecular pump is a main type now. It works on a principle that gas molecules can be deflected in

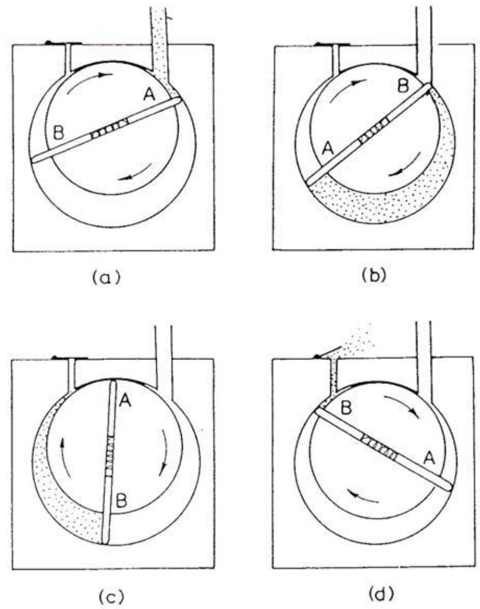

Figure 3.2: Schematic diagram of a rotary vacuum pump [4]

a desired direction by a collision with a spinning turbine rotor. By using the turbomolecular pump, an ultra-high vacuum (10^{-8} Pa) can be achieved.

An ion pump ionizes gas by the means of strong electrical potential (typically units of kV) and captures ions by a solid electrode. They are commonly used near the specimen and the electron gun, because they are compact and a pure, ultra-high vacuum can be achieved.

3.2 Scanning electron microscope

A scanning electron microscope (SEM) based on the secondary emission of electrons was developed at the RCA Laboratories in New Jersey during the Second World War. Unlike the TEM, where electrons are transmitted through a thin specimen, the SEM is used to display a surface of the specimen. A schematic diagram of a SEM can be seen in Figure 3.4.

The maximum accelerating voltage is lower than for a TEM (typically 30 kV) [4]. It results in a smaller electron gun and smaller magnetic lenses. There are also fewer lenses used, because imaging lenses are not required.

The electron beam of a SEM scannes the specimen in two perpendicular directions. The x-scan is fast and is generated by a sawtooth-wave generator connected to two coils, that deflect the electron beam. The y-scan is much slower and is generated by a second sawtooth-wave generator. This procedure is known as raster scanning and covers a rectangular area of the specimen. An image of the specimen is usually created by the detection of secondary emissioned or backscattered electrons.

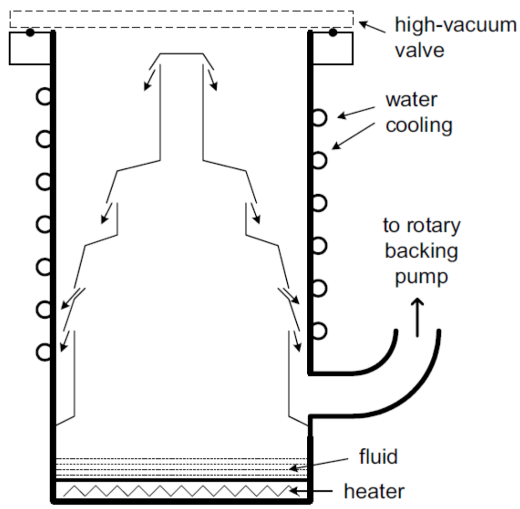

Figure 3.3: Schematic diagram of a diffusion pump [4]

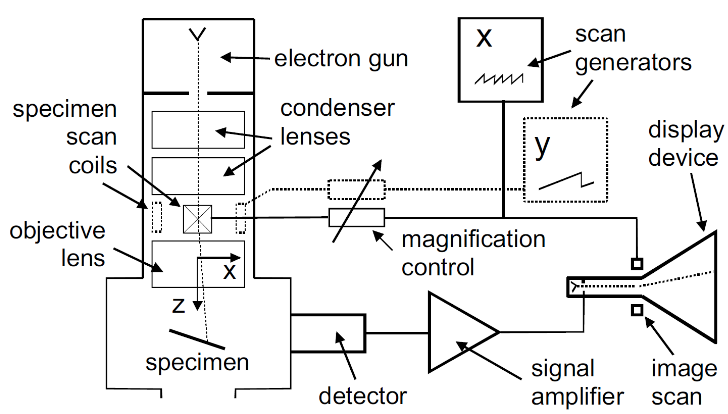

Figure 3.4: Schematic diagram of a scanning electron microscope [4]

Chapter 4

Pixel Detectors

Pixel detectors have many of advantages, such as small dimensions, good energy resolution, fast timing or cheap fabrication.They are used in many areas, such as medical imaging or high energy particle physics.

4.1 The p-n Junction as a Detector

The p-n junction (Fig. 4.1) is well-known for its role as a diode. The junction conducts current when a voltage is applied in the “forward” direction (positive voltage is applied to the p side), but it will conduct very little current when biased in the “reverse” direction. In the “forward” direction, the majority charge carriers migrate through the junction, which the current flows through and therefore cannot be used as a detector.

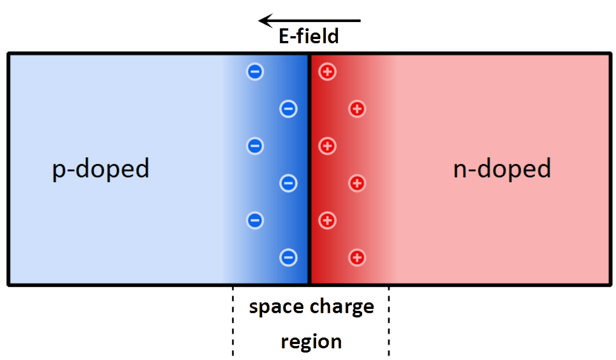

Figure 4.1: The p-n junction

However, when a reverse voltage is applied, a depletion zone, which is sensitive to the passing of charged particles, is created. The total width of the depletion region d can be expressed as:

$$d \cong \sqrt{2\varepsilon_r\varepsilon_0 V \mu \rho_D}, \tag{4.1}$$

where V is the applied bias voltage, μ is the mobility of the majority charge carriers and ρ_D is the resistivity of the doped semiconductor. As can be seen, the largest depletion width for a given voltage can be achieved by using a material with the highest resistivity. This resistivity is limited by the purity of the undoped material. Therefore, it is important to make detectors from the highest purity material available.

4.2 Pixel Detector Fabrication

In this section, the key steps of detector fabrication will be discussed. This process is derived from the planar technology developed for microelectronics and thus profits from its research. An example of production can be seen in Figure 4.2 and will be described below.

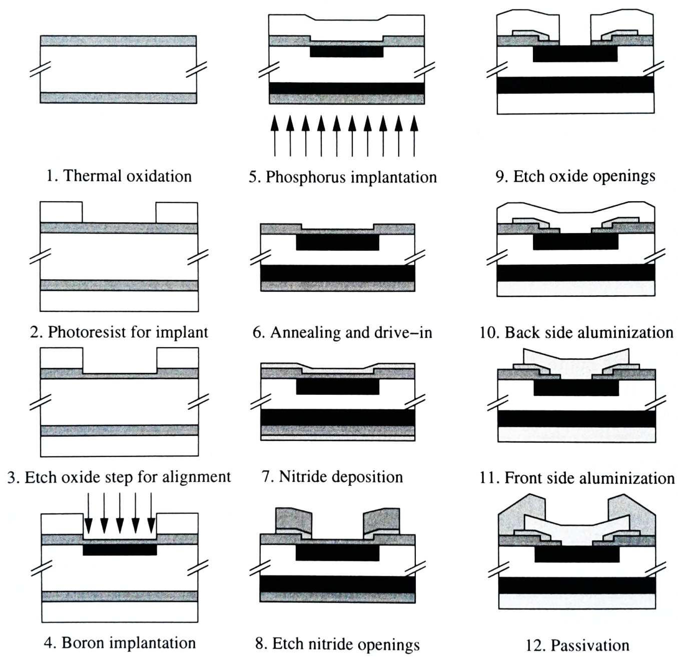

Figure 4.2: An example of production of a sensor. [10]

4.2.1 Wafer Production

The first step is the production of wafers. Silicon is isolated from quartzite by reduction with carbon at temperatures above 1400°C. This silicon is then converted to form trichlorosilane ($SiHCl_3$) and boiled. The boiling point of impurities is higher, so trichlorosilane is cleaned and transformed back to solid silicon. This material is used to grow large crystals. There are two common growing methods.

The Czochralski method can be seen in Figure 4.3. The silicon melt is contained in a crucible. A seed crystal is pulled under rotation from the surface of the liquid. Silicon freezes out at the surface. The diameter of an ingot can be modified by the speed of rotation.

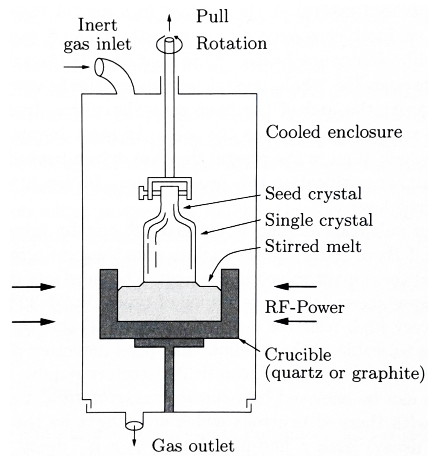

Figure 4.3: Schematic diagram of a Czochralski process. [10]

However, the Czochralski-grown silicon can not be used for applications requiring resistivity higher than 10 Ωcm because of many impurities [10].

Detectors, for which a high resistivity is needed, can be produced using the float zone (FZ) method. As shown in Figure 4.4, a high-purity silicon rod is vertically mounted in an inert gas atmosphere. A small zone of the rod is melted by the radio-frequency heater. This is called the float zone and it is moved from the seed crystal to the top by moving the RC heater slowly upward and the silicon freezes out as a single crystal. Since most impurities are better solvable in the melt than in the crystal, they are driven toward the end of the ingot [10]. This process can be repeated several times for further purification.

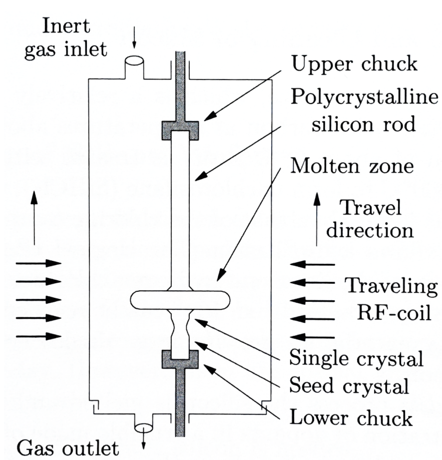

Figure 4.4: Schematic diagram of a float zone process. [10]

The crystal ingots are cut into wafers which are lapped and polished. The typical thickness of these wafers is around 300 μm.

4.2.2 Thermal Oxidation

The next step is usually thermal oxidation of the wafer surface (Figure 4.2-1.). Silicon oxide is grown by storing the wafer at a high temperature (between 900 and 1200°C [11]) in an oxygen atmosphere. It is called dry oxidation. If a faster growth is required, water vapor is added to the atmosphere, this process is called wet oxidation. However, slow growth usually provides quality in breakdown stability, surface changes and other properties. Thin gate oxides in the MOS electronics are usually grown at a lower temperature (around 800°C [10]).

Thermal oxidation provides protection of the wafer surface and also provides good termination of the silicon crystal. [10]

4.2.3 Patterning

For patterning of a wafer, a technique called photolithography is used. A photo-sensitive material (photoresist) is dropped in the center of the wafer and is distributed by fast rotation of the wafer. Photoresist is illuminated through a mask, usually a chrome pattern on a glass substrate. For a good resolution, a short wavelength in the UV range is used. Then the illuminated areas (positive resist, more common) or nonilluminated areas (negative resist) are removed, and therefore exposed to etching or implantation.

4.2.4 Etching

Copying the structure of the photoresist into the underlaying layers and removing the material is done by etching. There are two types of etching, wet etching and dry etching.

Wet etching is commonly used in sensor processing. The wafer is immersed in a bath. This leads to an underetching of the mask; however, it is not a problem due to the relatively small sizes.

In microelectronics, dry plasma etching is the most widely used method. It provides a high degree of anisotropy, and therefore allows creation of small structures unlike the wet etching. However, the plasma induces radiation damage in the oxides, so this process is inappropriate for the sensor technology.

4.2.5 Doping

There are two methods to introduce dopants into the silicon surface - diffusion and implantation. Boron is the most common p-dopant, whereas phosphorus and arsenic are typical n-dopants.

Diffusion

During diffusion doping, the wafer is exposed to dopants in the form of gas at the temperature of 800-1200°C [10]. Higher temperatures accelerate the diffusion process, so the depth of doping depends on the duration, concentration and temperature.

Ion Implantation

Ion implantation is currently the most commonly used doping method. The doping atoms are ionized, accelerated by an accelerator (10-15 kV [8]) and shot into the silicon wafer. The penetration depth of the ions and the shape of the doping profile can be adjusted by choosing an appropriate accelerating voltage.

After implantation, ions are placed in interstitial sites of the crystal lattice, so they are not electrically active. In addition, the crystal is damaged by the implantation, thus thermal annealing is required. However, the temperature (500°C [8]) is substantially lower than the temperature required for diffusion, so the material is not as damaged as by the diffusion process.

4.2.6 Metallization

Metallization (Figure 4.2-10.,11.) provides a low resistivity connection between devices on the same silicon substrate. The most common metal used for metallization is aluminium (aluminization process), because of its low resistance and its good adhesion on silicon oxide [10]. The metal can be sputtered or evaporated. A good ohmic contact is possible only if the silicon is highly doped on the contact. Also a sintering step is necessary.

4.2.7 Surface Passivation

The final step of detector production is usually surface passivation (Fig. 4.2-12.). The silicon surface must be protected against mechanical damage and chemical contamination. Thermally grown silicon dioxide is ideal for this purpose. It is used for the gate insulator in metal oxide semiconductor field effect transistors (MOSFETs) and as the surface passivation between strip or pixel detectors, where it is a crucial step.

Oxides can be thermally grown by a process called chemical vapor deposition - the wafers are exposed to gaseous ambient in high temperature furnaces.

4.3 Charge Coupled Devices

Charge coupled devices (CCDs) were introduced in 1969 by Williard Boyle and George E. Smith for recording of visible light. However, they can be extremely useful as sensors for radiation detection and imaging.

A schematic diagram of a simple linear CCD can be seen in Figure 4.5. The thickness of a CCD is usually few hundreds of microns. A depletion region is created below the front surface, and a potential minimum for electrons is created a few microns below the surface, which consists of a metal-oxide-silicon (MOS) electrode structure or a p-n diode structure.

The expansion of CCDs arises from its simple serial readout technique. After the exposure period, drive pulses are applied on the control electrodes and the accumulated electrons are shifted in a preferred direction. This is done by using three drive lines. The trapped electrons are collected by an anode at the edge of the wafer.

A two dimensional detector is obtained by attaching a couple of linear CCDs in parallel, which are readout by another linear CCD as illustrated in Figure 4.6.

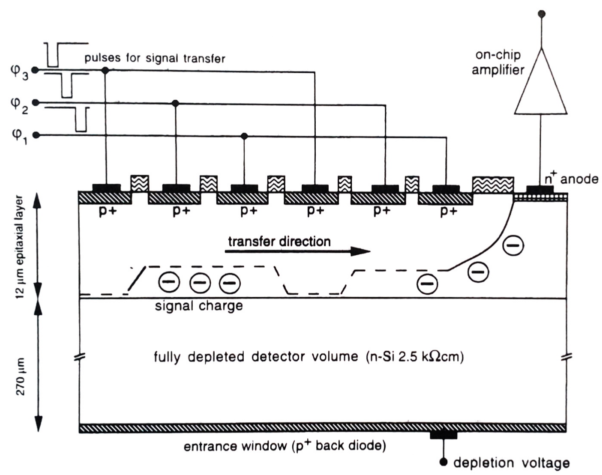

Figure 4.5: A schematic diagram of a linear CCD chip. [6]

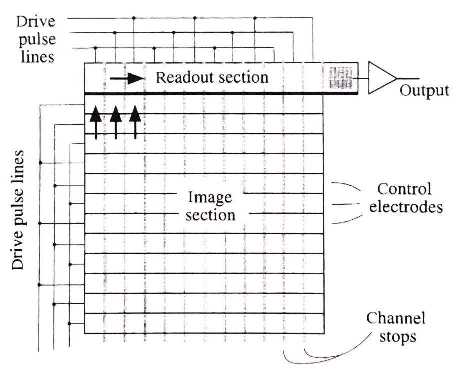

Figure 4.6: Layout of a two-dimensional CCD. [6]

For noise suppression, readout time of about 10 μs per pixel is needed. This implies the maximum readout rate of about 10^5 pixels per second. However, the readout mode described above is inapplicable in case of large area CCDs, which can contain more than 10^6 pixels. One approach to speeding up the readout is to divide the image section into several parts and read them out separately. Another approach involves storage in a second area of the CCD to allow resetting of the image section.

During the readout, there is also a smearing problem. During the readout phase, charges are in the process of moving from pixel to pixel and additional hits will be registered in the wrong position. For weakly penetrating particles, a shutter can be used during the readout phase. However, this solution can not be used for more penetrating particles. Another solution is to minimize the readout time in comparison with the exposure time, which results in a higher noise level.

4.4 Medipix

Medipix is a family of chips developed by an international collaboration because of the needs of the Large Hadron Collider experiments at CERN. The activity of this collaboration started in the 1990's with a Medipix1 detector (or Photon Counting Chip) to provide a noise-free single photon counting. At the end of the 1990's, Medipix2 collaboration was formed to design a new chip with reduceed the pixel size and increased number of pixels per chip. Another chip developed within the Medipix2 collaboration was Timepix. In the Timepix chip, pixels can count hits like Medipix2 or work in a Time-Over-Threshold mode to provide a rough energy information. In 2006, Medipix3 collaboration was formed to improve the energy resolution and continuous readout.

4.4.1 Medipix2 Chip

Medipix2 is a hybrid pixel detector consistiong of a sensor and readout electronics. These two layers are bumb-bonded together as can be seen in Figure 4.7. Placing the periphery at the bottom of the chip results in minimizing of the non-sensitive area of the detector.

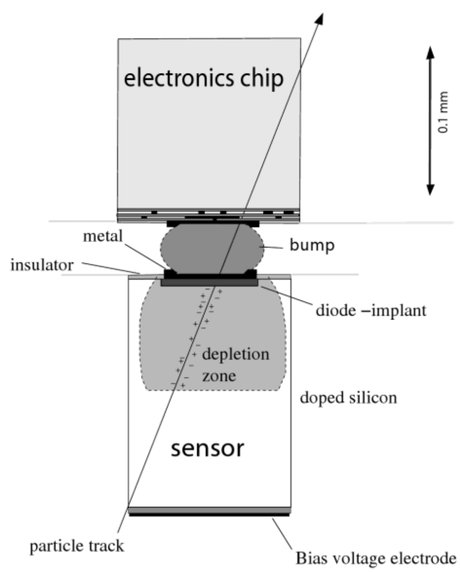

Figure 4.7: Schematic diagram of the hybrid pixel detector [10]

The Medipix2 pixel detector consist of a matrix of 256×256 identical elements. The surface area of each element is $55\,\mu\text{m} \times 55\,\mu\text{m}$ and contains 504 transistors and has a static power consumption of $\sim 8\,\mu\text{W}$. The whole chip contains around 33 million transistors and operates with 2.2 V power supply with a total analog power consumption of about 500 mW.

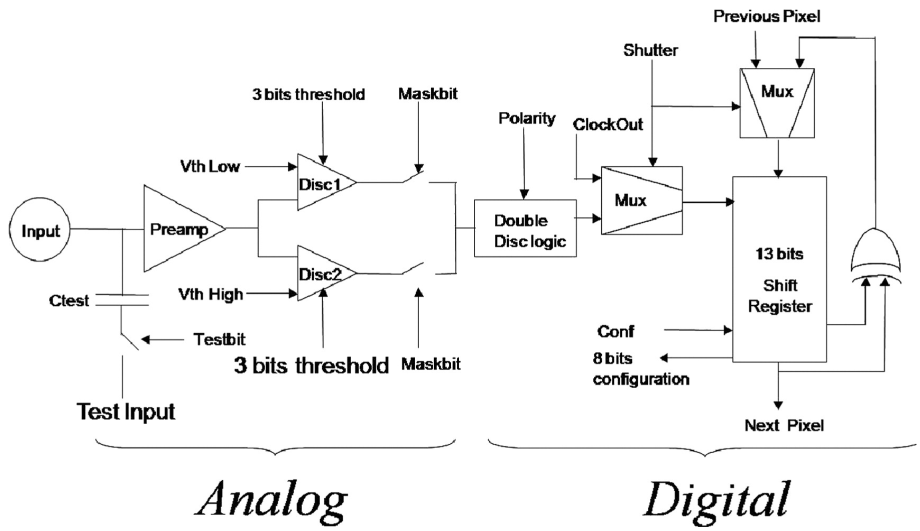

Figure 4.8: Schematic diagram of the Medipix2 pixel cell [2]

The Pixel Cell

Figure 4.8 shows a schematic of the Medipix2 pixel cell. Charged particles deposit a charge which drifts toward the collection electrodes. This charge is then preamplified. The output of the preamplifier is followed by two identical discriminators, which are independent and the discrimination energy can be set by THL and THH thresholds. The THL(THH) threshold contains a 4-bits THL(H)coarse, 10-bits THL(H)fine and 3-bit adjustment. The difference between the two energy levels defines the energy window. The output can be masked in case of malfunction or excessive noise by a maskbit. The double discrimination logic (DDL) can also work in single discrimination mode. The shift register can operate in two modes. When the Shutter is low, the shift register works as a 13-bit pseudo-random counter. When the Shutter is high, an external clock is used to shift data from pixel to pixel. This mode is used to set the 8 configuration bits and for reading the counter information.

The Periphery

The periphery contains 13 8-bit DACs which set the different voltage or current on the chip, a 256-bit fast shift register (FSR) for configuration or readout, 137 Input/output pads, high speed low voltage differential signaling (LVDS) drivers and receivers and IO logic that controls the chip. Using a 200 MHz clock, the chip can be read out within 5 ms through the serial port or using a 32-bit CMOS bus within 300 μs using a 100 MHz clock.

Readout Hardware

The first interface system between Medipix2 and commercial PCI bus was MUROS2 (Medipix re-Usable Read Out System) developed by Nikhef Amsterdam. It includes a readout card with power supplies and control circuitry and it is able to acquire about 25 frames per second (fps) using a single chip and about 5 fps using a quad (2×2 chips) assembly.

An USB readout system, developed by IEAP, CTU in Prague, has gained a great popularity among Collaboration members. It uses the USB 1.1 standard and therefore it is limited in readout speed to 5 fps for a single chip. The advantage of this readout system is its compactness and ability to provide a power supply as well as communication with Medipix2 chip in single or quad chip assembly.

Another option is a Relaxd module. Relaxd stands for: high-REsolution Large Area X-ray Detector. The module is designed such that it is possible to 'tile' the Medipix devices of multiple Relaxd modules into one larger active area. The module is controlled and read out via a 1Gbit (electrical) Ethernet connection using TCP/IP UDP messaging, allowing a direct connection to a standard PC. [12]

Readout Software

Pixelman is a software package for Medipix2 acquisition control. It supports all available Medipix2 based devices (Medipix 2.1, Medipix2 MXR, Timepix, Medipix 2.1 Quad, Medipix2 MXR Quad, Timepix Quad) and commonly used readout interfaces - MUROS2 and USB readout interfaces. It is designed for maximum flexibility and interoperability with other devices to make possible to control complex experiments. This is achieved by modular architecture with the support of custom made plugins. [3]

Chapter 5

Medipix in Electron Microscopy

5.1 Installation of Medipix

In cooperation with the Institute of Physics of the Academy of Sciences of the Czech Republic (ASCR), an electron microscope in Cukrovarnická laboratories was chosen for this research. The measurement was performed using a Philips CM120 transmission electron microscope, which can be seen in Figure 5.1. It is equipped with a standart CCD camera; however, a Medipix detector can provide a better dynamic range and radiation hardness.

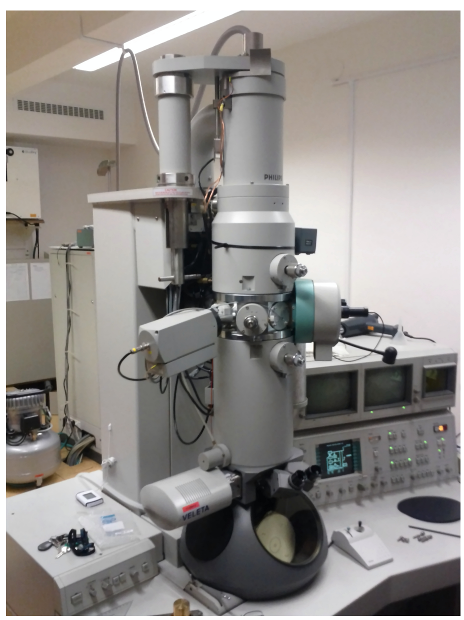

Figure 5.1: An electron microscope at the IoP ASCR - Philips CM120

It was decided to place our Medipix detector in the bottom position, under the fluorescent

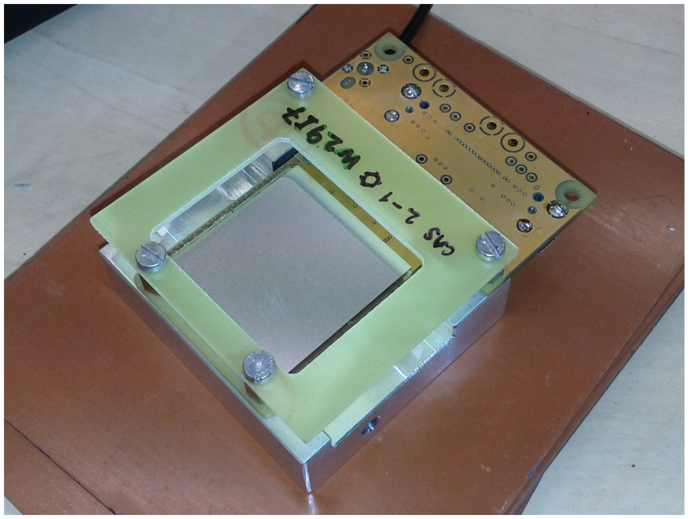

Figure 5.2: A quad Medipix chip layout

screen. The reason was a relatively easy access and the possibility to use the Medipix and a CCD Camera at the same time.

Figure 5.2 shows our Medipix quad chip with aluminium radiator and SCSI VHDCI 68-pin connector. The first problem that had to be solved was to ensure the cable connection into the vacuumed volume of the microscope. A special flange with a vacuum feedthrough was made. The detector was placed on the metal plate, which was screwed to the base of the microscope to ensure the thermal connection.

After evacuation and switching the microscope on, the detector was connected to the notebook and set for readout. Several images have been obtained; however, after a few minutes the detector began to overheat and the measurement had to be stopped or the chip would be irreparably damaged. The power consumption of our Medipix varies in the range from 2 W to 5 W and this energy is released as heat. The thermal connection between the detector and the microscope has proved insufficient and another way of cooling must be invented.

However, several pictures have been obtained during the measurement and it was found that the Medipix2 chip has a much better contrast than the CCD camera. Moreover, its radiation hardness allows an operation without the direct beam shielding.

5.2 Image Corrections

5.2.1 Pixel Layout

Our test device was a Medipix2 chip in a quad chip assembly. As can be seen in Figure 5.3 there is a special pixel layout. At first, there are hexagonal pixel cells, which are shifted by a half pixel in rows relative to each other. There are also oblong pixel cells at the edges to cover the area between chips. The length of these pixels is twice their width. The size of the middle four pixels is two times greater in both directions to cover the whole area. Lastly, pixels at both

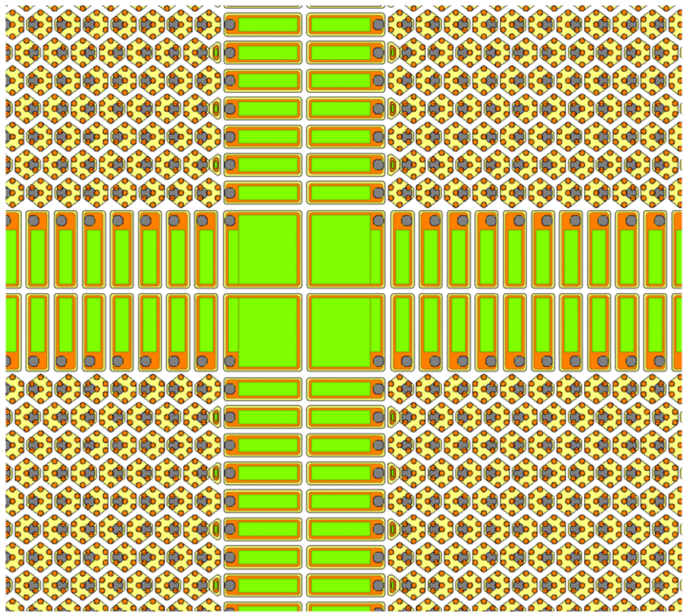

Figure 5.3: A quad cross detail [13]

ends of every second row have a half or one and a half lenght.

5.2.2 Image Defects and Their Corrections

The Borderline of Chips

As is shown in Figure 5.4, the untypical dimensions of pixels at the border of chips result not only in a wrong position of image, but also in an overexposure of these pixels due to more hits in pixels. The former can be easily fixed by inserting another two rows of pixels of the same color in the appropriate direction. The latter can be solved by dividing the number of hits in these pixels by their relative size. However, a better solution has been proposed by assuming, that the sum of exposures in these pixels is similar to the sum of exposures in the neighboring row of pixels and the overexposure pixel can be rescaled by the fraction of these sums. The four central pixels were then rescaled using the closest pixel on the diagonal. The result of these considerations can be seen in Figure 5.4.

Hexagonal Pixels

As was mentioned above, using hexagonal pixels results in a better resolution of the detector, because hexagonal pixels are a circle more than the square pixels, so the edges of the image that are not horizontal or vertical are much smoother. However, it is not easy to properly display the image in a square pixel matrix. To achieve the right position of pixels, the hexagonal pixels have been replaced by square pixels and the even rows have been shifted by a half cell. Therefore, each hexagonal pixel has to be replaced by four identical square pixels and then shifted by one pixel. The comparisson of this correction to the original image can be seen in Figure 5.5.

An example of the image before and after all corrections is shown in Figures 5.6 and 5.7.

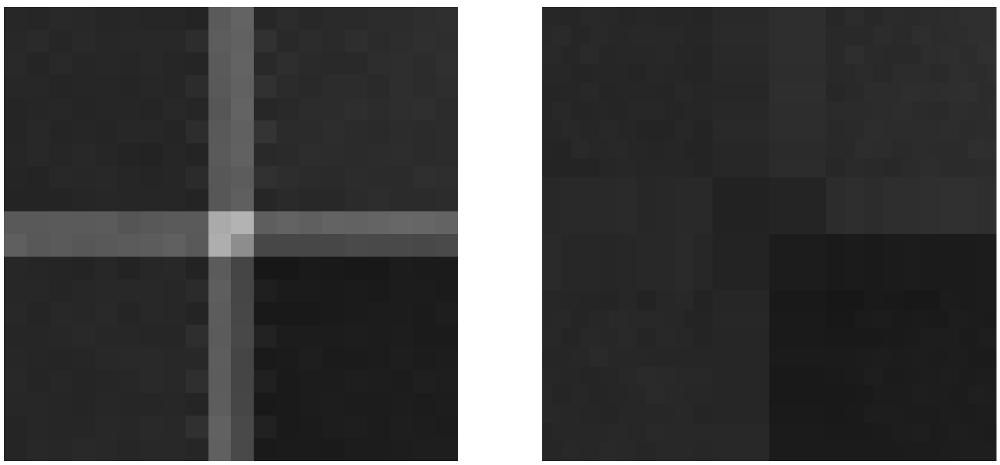

Figure 5.4: Left: The middle of an original image. Right: The same place after correction.

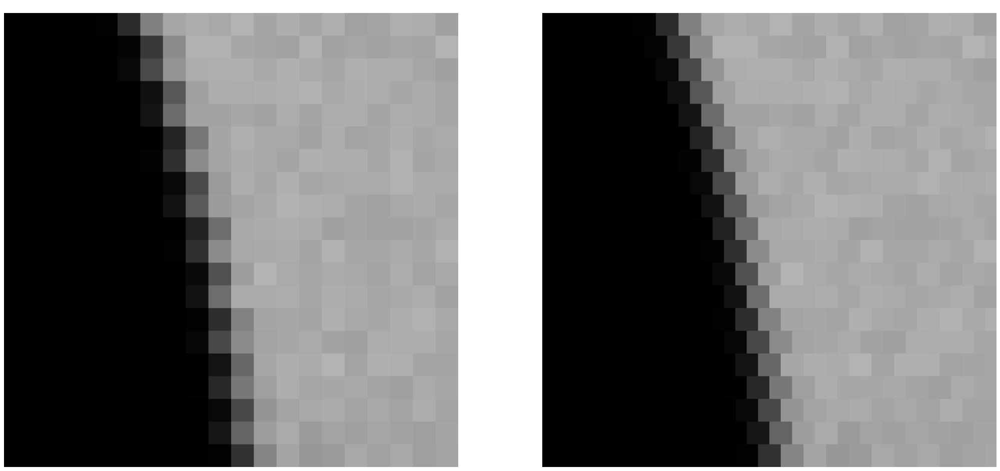

Figure 5.5: Left: An edge in the image before correction. Right: The edge after correction.

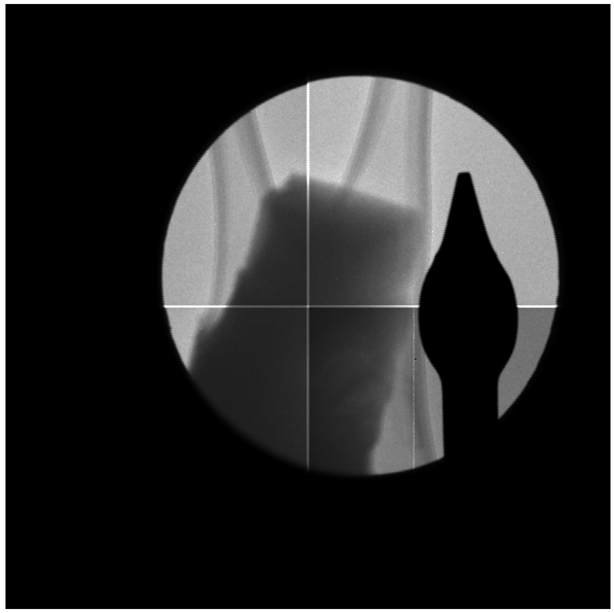

Figure 5.6: An example of the image before corrections

Figure 5.7: An example of the image after corrections

5.3 A graphical user interface

To expedite and simplify the creation of corrected images, a Windows C++ application with a graphical user interface (GUI) in a Dev-C++ [1] was developed. It is a free integrated development enviroment written in Delphi and using a MinGW compiler.

A layout of the application is shown in Figure 5.8. There is an “Open” button that allows the user to choose a .txt file, from which an image will be created. Below this button there are two edits. These boxes are used for setting the contrast of the image. There is also a “Create original” checkbox, which creates an uncorrected image. Finally, the “Create” button runs the process of correction and saves the image on the harddrive.

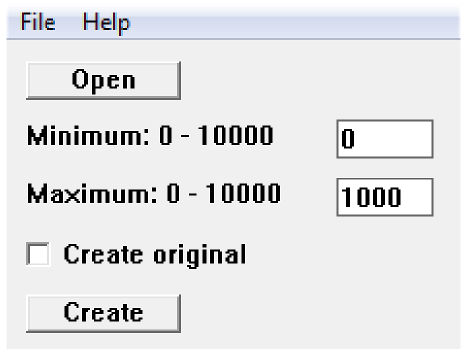

Figure 5.8: A graphical user interface of the application for image corrections

The data are loaded from a .txt file into a matrix. In case of a quad detector, four matrices (one for each chip) of dimensions 256×256 are created. The reason is to make the code as simple as possible, and even though the chips are identical, they are inverted along the axis and it would be difficult to work with one large matrix. Then the overexposed pixels are changed. Next, the dimensions of the borderline pixels are fixed by an enlargement of the matrix to 258×258 pixels, as was mentioned above. After that, the matrix is again enlarged to 516×516 pixels and the data are properly shifted to achieve the right position of hexagonal cells. Then the four matrices are put together into a large 1032×1032 matrix. At the end, the integer values in matrix must be changed to 16-bit and written as a 16-bit .png image using the libpng library [9] in 1032×1032 resolution.

Chapter 6

Summary

The purpose of this work was to examine new possibilities of the image registration in the transmission electron microscope and determine their advantages over the common CCD camera.

The Medipix2 detector was placed in the bottom position of the microscope, under the fluorescent screen. The cable connection was ensured by a special flange with a vacuum feedthrough into the vacuumed volume of the microscope. Due to the detector overheating, the measurement had to be stopped or the chip would be irreparably damaged. The thermal connection between the detector and the microscope has proved insufficient and another cooling mechanism must be introduced.

The image defects caused by the connection between chips and by the hexagonal pixel cell were corrected, as mentioned in the last chapter. A special C++ application with a graphical user interface was created to expedite and simplify the creation of corrected images.

This work is a preparation for a further research of the Medipix2 detector application in the electron microscopy. During this work I expanded my knowledge of electron miscoscopy and Medipix detectors, and I gained a lot of experience in C++ programming.

Bibliography

[1] Bloodshet. Dev - c++. http://www.bloodshed.net/devcpp.html, [online 24.8.2014].

[2] Campbell, M. 10 years of the medipix2 collaboration. *Nuclear Instruments & Methods in Physics Research A 663* (2011).

[3] Daniel Tureček, Tomáš Holý, Z. V. Pixelman. http://aladdin.utef.cvut.cz/ofat/others/Pixelman/index.html, [online 29.7.2014].

[4] Egerton, R. F. *Physical Principles of Electron Microscopy: An Introduction to TEM, SEM, and AEM.* Springer, 2005.

[5] Karlík, M. *Úvod do transmisní elektronové mikroskopie.* Česká technika, 2011.

[6] Knoll, G. F. *Radiation Detection and Measurement*, 3rd ed. John Wiley and Sons, 2000.

[7] Krumeich, F. Properties of electron, their interaction with matter and applications in electron microscopy.

[8] Průša, P., and Gerndt, J. *Detektory ionizujícího záření.* Česká technika, 1995.

[9] Roelofs, G. libpng home page. http://www.libpng.org/pub/png/libpng.html, [online 24.8.2014].

[10] Rossi, L., et al. *Pixel Detector: From Fundamentals to Applications.* Springer, 2006.

[11] Spieler, H. *Semiconductor Detector Systems.* Oxford University Press, 2005.

[12] Vincent van Beveren, Henk Boterenbrood, M. H. Relaxd module. https://lbtwiki.cern.ch/pub/VELO/VeloTestbeam2012/Relaxd-manual.pdf, [online 10.9.2014].

[13] Vrba, V. Medipix sensors from on semiconductor. PDF presentation, September 2006.